TITLE: **MODELING DDT IN GRANULAR EXPLOSIVES WITH A MULTI-MATERIAL HYDROCODE**

AUTHOR(S): **Edward M. Kober, T-14, LANL**
John B. Bdzil, DX-10, LANL
Stephen F. Son, DX-16, LANL

Los Alamos

Los Alamos National Laboratory
Los Alamos, New Mexico 87545

MODELING DDT IN GRANULAR EXPLOSIVES WITH A MULTI-DIMENSIONAL HYDROCODE *

E. M. KOBER, J. B. BDZIL and S. F. SON

Los Alamos National Laboratory, Los Alamos, New Mexico 37545 USA

We describe results obtained with the implementation of a new large drag limit, two-phase continuum mixture model of DDT into MESA-2D. The kinetics scheme originally described by BN is used to simulate a suite of 1D and 2D experiments. The BN kinetics scheme is found to be inadequate.

INTRODUCTION

When an explosive sustains damage due to an impact, its porosity can increase which makes it very sensitive to accidental initiation of detonation by both subsequent weak impacts and thermal sources. As part of the explosive safety program at Los Alamos, our group has worked to develop models for compaction wave supported ignition of granular explosives, and to implement these model in hydrodynamics codes. The pre-existing models of deflagration-to-detonation transition (DDT) were examined as part of our work, especially the Baer & Nunziato (BN) model (1), and new models were developed. Here we report on the implementation of a new large drag limit, two-phase continuum mixture model that we have developed (2).

This model is an outgrowth of our studies of the role played by having different solid and gas velocities in compaction driven combustion (3) (4). We find that because the interphase drag is high in low porosity (~ 30%) materials, large O(1) differences in the velocity are principally found in the narrow zone that comprises a two-phase shock. Elsewhere in the flow, velocity differences are small and effectively approximated by a combined pressure-density gradient term. Although thin, this drag-relaxation zone does not integrate to a simple jump condition, a structure problem needs to be solved. We have developed a viscous model that properly regularizes this zone. This very thin zone was not properly resolved in earlier work (1) & (5). When it is not

properly resolved, properties of the numerical algorithm can determine the energy partition between phases, and not the physics.

We have implemented our model in the MESA hydrodynamics code (6). One version of the implementation uses the phase interaction terms and rate laws described by BN (5). Here we report that the BN model does not reproduce the qualitative trends of a suite of new one-dimensional (1D) experiments on granular HMX. We also describe two dimensional (2D) simulations of the DDT tube test, and illustrate the important role played by multimaterial, multidimensional simulations in interpreting the relatively slow process of DDT.

MODEL

The basic hydrodynamic equations of our two-phase, large drag model consists of separate phase mass and energy conservation equations, a single mixture momentum equation and an equation for the volume fraction (7): (1)

$$\frac{D}{Dt}(\varphi_s \rho_s) + \varphi_s \rho_s \vec{\nabla} \cdot \vec{u} = C \tag{1}$$

$$\frac{D}{Dt}(\varphi_g \rho_g) + \varphi_g \rho_g \vec{\nabla} \cdot \vec{u} = -C \tag{2}$$

$$(\varphi_s \rho_s)\frac{D e_s}{Dt} + \varphi_s P_s \vec{\nabla} \cdot \vec{u} = \mathcal{E}_s \tag{3}$$

$$(\varphi_g \rho_g)\frac{D e_g}{Dt} + \varphi_g P_g \vec{\nabla} \cdot \vec{u} = \mathcal{E}_g + (e_s - e_g)C \tag{4}$$

$$\frac{D u}{Dt} + \frac{1}{\rho}\vec{\nabla} P = 0 \tag{5}$$

$$\frac{D \varphi_s}{Dt} = F + \frac{C}{\rho_s} \tag{6}$$

Subscripts s and g refer to the solid and gas phase, respectively. The state variables are density (ρ_i), specific internal energy (e_i), pressures (P_i), particle velocity (u_i), temperature (T_i), and volume fraction (ϕ_i) where i is s or g. The mixture variables are the mixture density ($\rho = \phi_s\rho_s + \phi_g\rho_g$) and mixture pressure ($P = \phi_s P_s + \phi_g P_g$). The saturation constraint is $\phi_s + \phi_g = 1$. The source terms appearing above are rate of compaction ($\mathcal{F}$), interphase energy exchange ($\mathcal{E}$), and volumetric rate of mass exchange ($\mathcal{C}$). The Lagrangian derivative is $D/Dt \equiv \partial/\partial t + \vec{u} \cdot \vec{\nabla}$.

We have analyzed the structure of two-phase, two-velocity shocks in the limit of large drag (4). Based on these results, we have developed the following regularization for shocks

$$P_g \Rightarrow P_g + \left(\frac{\nu_r \rho_g}{\rho + \phi_g \rho_g (\nu_r - 1)} \right) Q, \qquad (7)$$

where the regularization constant, ν_r, sets the partition of energy between the solid and gas. Q is the viscous pressure for the mixture (Q is taken as the artificial viscosity used by the code).

The Hayes equation of state (EOS) is assumed for the solid (e.g., (1)).

$$T_s(e_s, \rho_s) = T_{s0} + \frac{e_s}{C_{vs}} \qquad (8)$$

$$+ \frac{1}{C_{vs}}\left((t_3 - P_{s0}/\rho_{s0})(1 - e_s) + G(e_s; t_4)\right).$$

$$P_s(T_s, \rho_s) = P_{s0} + (T_s - T_{s0})C_{vs}g_0 + \rho_{s0}dG/de_s, \qquad (9)$$

where $G(e_s; t_4) \equiv -t_4[e_s^{1-n} - (n-1)(1 - e_s) - 1]$ and $e_s \equiv \rho_{s0}/\rho_s$. The Jones-Wilkins-Lee (JWL) EOS is assumed for the gas (e.g., (1)).

$$T_g(e_g, \rho_g) = T_{g0} + \frac{1}{C_{vg}}(e_g + \Delta H) \qquad (10)$$

$$- \frac{1}{C_{vg}\phi_{s0}\rho_{s0}}\left(\frac{A(\rho_g)}{R_1} + \frac{B(\rho_g)}{R_2}\right).$$

$$P_g(T_g, \rho_g) = T_g \omega C_{vg} \rho_g + A(\rho_g) + B(\rho_g), \qquad (11)$$

where $A(\rho_g) \equiv A\exp(-R_1\phi_{s0}\rho_{s0}/\rho_g)$ and $B(\rho_g) \equiv B\exp(-R_2\phi_{s0}\rho_{s0}/\rho_g)$.

Interaction Terms

There are some notable inconsistencies in the form of $\mathcal{E}$. BN's published expression is $\mathcal{E} = -(P_s - \beta_s(\phi_s))\mathcal{F} - \mathcal{H}(T_s - T_g)$, where the first term is a model for the compaction related work and the second term models interphase heat transfer. The BN calculations (5) used $\mathcal{E} = -\mathcal{H}(T_s - T_g)$. Our suggested form is $\mathcal{E} = -P_g\mathcal{F} - \mathcal{H}(T_s - T_g)$ which corresponds to depositing the compaction work with the solid (2). Here we use the former expression to maintain compatibility with BN's calculations.

The BN compaction law is (1):

$$\mathcal{F} = \frac{\phi_s\phi_g}{\mu_c}(\max(P_s - \beta_s, 0) - P_g). \qquad (12)$$

where μ_c is the compaction viscosity. The intragranular stress or configuration pressure, β_s, is $\beta_s = -\max[(\phi_s - \phi_{s0}), 0]\tau\ln(\phi_g)/\phi_g$.

The volumetric heat transfer coefficient, $\mathcal{H}$, is assumed to have the form, $\mathcal{H} = (3k_g\phi_s)/(a_p^2)$ where a_p is an effective particle radius assumed to be simply related to ϕ_s, $a_p = a_{p0}\max(1, (\phi_{s0}/\phi_s)^{1/3})$ in BN's calculations. Although the results are insensitive to this dependence, the intended relationship was $a_p = a_{p0}\min(1, (\phi_s/\phi_{s0})^{1/3})$.

Kinetics

We use the BN kinetics scheme described in(5). Then $\mathcal{C}$ is a model for gas phase combustion, modified with switches that attempt to impart the flavor of a compaction supported ignition mechanism, via an induction variable, I and a grain surface temperature, ζ. The induction time equation is

$$\frac{DI}{Dt} = k_I((P - P_0)/P_0)^2(1 - I). \qquad (13)$$

where $0 \leq I \leq 1$. This equation is simply a timer that triggers a change in the gas energy reference state (combustion energy release), ΔH, given by $\Delta H = (1 - H(I - 1/2))\Delta H_{pur} + H(I - 1/2)\Delta H_{det}$. The surface temperature equation is,

$$\frac{D\zeta}{Dt} = \mathcal{H}(T_g - T_{int})/(C_{vs}\phi_s\rho_s). \qquad (14)$$

where $\zeta(T_{int}, T_g, T_s)$ is a function of the interface temperature T_{int}. This function can be inverted to give,

$$T_{int} = \frac{5(\zeta + T_s) + BiT_g}{(5 + Bi)(1 + Bi)} \qquad (15)$$

$$+ \frac{Bi\left(T_s - Bi\zeta + \sqrt{Z^2 - |T_g - T_s|^2}\right)}{(1 + Bi)}.$$

where $Z \equiv \max(Bi\zeta/2, 0) + |T_g - T_s|$. We use $Bi \equiv 10k_g/k_s$, as in BN's calculations (5). This equation was derived assuming that interphase heat transfer is driven only by $(T_g - T_{int})$, and so neglects the heat generated by compaction. This interface temperature is used only to trigger the principal reaction in C.

$$C = -3H(T_{int} - T_{ign})k_p\left(\frac{P_g}{D_p}\right)^{b_n} \frac{\phi_s\rho_s(1 - f)^{2/3}}{a_p}$$

$$- k_h((P - P_0)/D_p)^2\rho_s(1 - \phi_{s0})f, \qquad (16)$$

where $f \equiv \max((\phi_s - \phi_{s0}), 0)/(1 - \phi_{s0})$ and k_p and k_h are rate constants.

The parameter values used by BN to model coarse grain granular HMX (class D) at $\phi_{s0} = 0.73$ are given in Table 1.

Table 1. Parameters for $\phi_{s0} = 0.73$, granular HMX.

$\Delta H_{det} = 7.796 \times 10^6$ J/kg	$C_{vg} = 2380$ J/kg/K
$\Delta H_{pyr} = 2.3 \times 10^6$ J/kg	$C_{vs} = 1500$ J/kg/K
$t_A = 4.97 \times 10^5$ J/kg	$\tau = 1.2 \times 10^7$ Pa
$t_4 = 8.24 \times 10^4$ J/kg	$k_f = 2 \times 10^4$ s^{-1}
$b_n(P_g < 69\,MPa) = 1.0$	$k_h = 100$ s^{-1}
$b_n(P_g \geq 69\,MPa) = 0.8$	$n = 9.8$
$k_p(P_g < 69\,MPa) = 0.1227$ m/s	$R_1 = 4.2$
$k_p(P_g \geq 69\,MPa) = 0.1139$ m/s	$R_2 = 1.0$
$a_f = 1.35 \times 10^{10}$ Pa	$\omega = 0.25$
$a_{p0} = 7.5 \times 10^{-5}$ m	$D_p = 10^8$ Pa
$A = 2.70 \times 10^{11}$ Pa	$T_{ign} = 525$ K
$B = -4.96 \times 10^8$ Pa	$\rho_{s0} = 1900$ kg/m^3
$k_g = 0.0943$ W/m - K	$g_s = 2100$ kg/m^3
$k_s = 0.423$ W/m - K	$\mu_s = 100$ kg/m - s

The regularization was $\nu_p = 1.0$ and $P_{s0} = P_{g0} = 10^5$ Pa, $T_{s0} = T_{g0} = 300$ K. Using these parameters all qualitative features were replicated

and fair quantitative comparison with BN's published calculations (5) were obtained. The ignition locus differed by a maximum of 4 μs through a 60 μs simulation. More favorable quantitative comparisons (to within numerical accuracy) have also been made with a 1D MacCormack's method based code integrating the large drag limit equations or the full BN equations (2-velocity) equations.

1D IMPACT SIMULATIONS

Sheffield et al. (8) have performed shock loading experiments on $\phi_{s0} = 0.73$, coarse grained, class A HMX (mean particle size of 1.5×10^{-4} m). The nominal sample thickness was 4×10^{-3} m, which is about 30 particle diameters. A sandwich geometry was used, where the HMX was surrounded by thick pieces of Kel-F or PMMA. The particle velocity was measured at both interfaces. A gas gun was used to shock load the samples, with the initial particle velocity at the interface ranging from $200-500$ m/s. Our 1D calculations used a grid size of $\Delta x = 2.5 \times 10^{-5}$ m. The comparison for Kel-F/HMX/PMMA when the initial projectile velocity is 390 m/s is shown in Fig. 1. For this case, I of Eq. (13) exceeds 0.5 at 7.5 μs (9.3 μs) for the left (right) gauge. The doubling of the pressure due to wave reflection (left) and impedance matching (right), leads to vigorous reaction at about 10 μs. The transit time of the compaction wave across the sample is 4 μs. A 2D simulation showed the flow becoming 2D on the centerline at about 9μs. The agreement of calculation with experiment is good.

When the initial input velocity is increased to 400 m/s, the experimental and computed velocity displayed in Fig. 2 show poor agreement. The cell transit time is 2μs, during which time as much reaction occurs as in 4μs for problem 1. This reflects the higher pressures in the system. However, the experiments show the reactions to be exponentially faster for this compared to the previous case. Thus the agreement is poor. Other cases in this suite of experiments show similar poor agreement with BN. Thus the BN reaction scheme inadequately represents the experiments. Similar results were obtained using the BN model integrated using a method of lines algorithm (9).
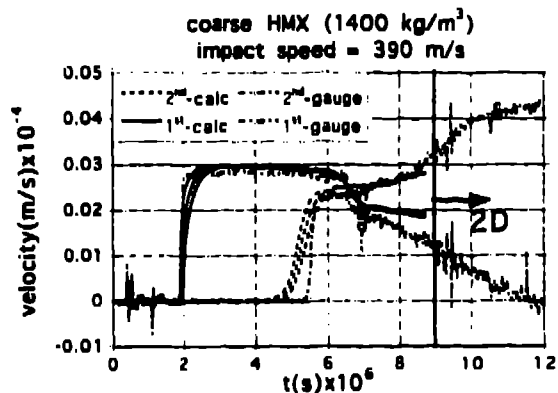
coarse HMX (1400 kg/m^3)
impact speed = 390 m/s

FIGURE 1. A comparison of experiments (dotted lines) and computed (solid lines) interface velocities. The computed compaction wave is too thick. The rounding of the computed velocity at the left interface is due to the time scale associated with the compaction process. However, the overall comparison is good.
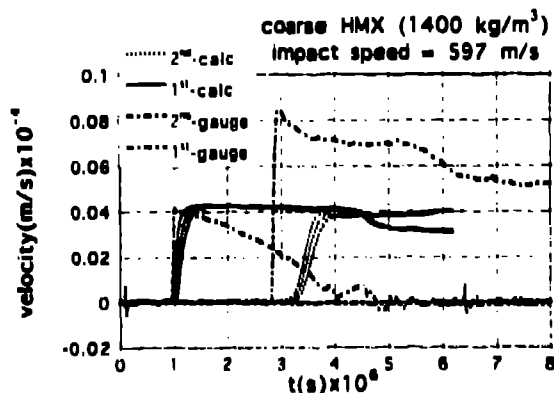

coarse HMX (1400 kg/m^3)
impact speed = 597 m/s

FIGURE 2. A comparison of experiments (dotted lines) and computed (solid lines) interface velocities. The agreement is poor.

2D "TUBE TEST"

A calculation of the "tube test" experiment performed by Sandusky & Bernacker (10) is shown in Fig. 3. The tube was Lexan (Johnson-Cook strength model) and the impactor rod, which initially was traveling at 207 m/s, was PMMA (fluid). Significantly, the large 2D effects bring into question 1D calibrations of models to such experiments. Models like BN were calibrated to such experiments using 1D simulations.
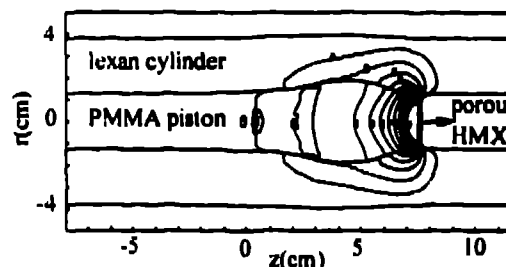

FIGURE 3. A calculation of Sandusky's 2D tube test. The pressure contours are shown.

CONCLUSION

The published BN "kinetics" scheme is fully described in this paper. It is both overly complex and *does not* provide an adequate representation of granular HMX. In addition to the discrepancies shown here, the "plug" that has been observed experimentally is not obtained. Work is ongoing in our group to develop better rate modeling. An initial effort in this direction is found in (11).

REFERENCES

1. M. R. Baer and J. W. Nunziato, in *Int. J. Multiphase Flow*, **12**, 861, (1986).
2. J. B. Bdzil et al., *in preparation*, (1995).
3. B. W Asay et al., *in preparation*, (1995).
4. J. B. Bdzil et al., *in preparation*, (1995).
5. M. R. Baer and J. W. Nunziato, in *Proc. 9th Det. Symp.*, 293, (1989).
6. K. S. Hollan et al., in *Proc. Supercomput. World Conf.*, (1989).
7. S. Passman, Int. J. Engng Sci. **15**, 117 (1977).
8. S. A. Sheffield et al., *in these proc.*, (1995).
9. J. B. Bdzil and S. F. Son Los Alamos Report *LA-12794*, (1995).
10. H. W. Sandusky and R. R. Bernacker in *Proc. 8th Det. Symp.*, 881, (1985).
11. S. F. Son et al., *in these proc.*, (1995)